

# Development of Microclimate Control Room using IoT System for Atmospheric Water Harvesting Research

Ronnachart Munsin<sup>1,\*</sup>, Autanan Wannachai<sup>1</sup>, Nopphadon Chongbun<sup>1</sup>, Satit Karnpian<sup>1</sup>, Nachapon Sumankant<sup>1</sup>, Kanthanat Sanwong<sup>1</sup>, Settawut Pinta<sup>1</sup>, Jirasak Panya<sup>1</sup>, Pracha Yeunyongkul<sup>1</sup>, Nawee Nuntapap<sup>1</sup>, Taweesak Mahawan<sup>1</sup>, Arpirak Hokpanna<sup>2</sup> and Nattaporn Chaiyat<sup>3</sup>

<sup>1</sup> Department of Mechanical Engineering, Rajamangala University of Technology Lanna, Huay Kaew Road, Muang, Chiang Mai 50300, Thailand

<sup>2</sup> Department of Mechanical Engineering, Faculty of Engineering, Chiang Mai University, Chiang Mai 50200, Thailand

<sup>3</sup> Thermal Design and Technology Laboratory (TDeT Lab), School of Renewable Energy, Maejo University, Nonghan, Sansai, Chiang Mai, 50290, Thailand

ronnachart@rmutl.ac.th\* (corresponding author)

**Abstract.** For testing the entire system of atmospheric water harvesting (AWH), large microclimate control room was required to provide the stable climate conditions. The objective of this work was to develop an innovative microclimate control room using IoT system to provide the realistic and stable situation for AWH research. A room with dimensions of  $2.5 \times 4.5 \times 3$  m ( $W \times L \times H$ ) was selected. Main controller units were used to collect data from a group of temperature and relative humidity sensors and to control microclimate through the operating devices, i.e. air conditioner, heaters, humidifier and dehumidifier. Modes of the control can be selected as offline control by the control panel or online control by the IoT platform. Flow and temperature distribution were assessed by computational fluid dynamics. The desired conditions at temperature and relative humidity between 20-45 °C and 40-80%, respectively, can be maintained by the control system with high stability. The alignment of the operating devices allowed homogeneous temperature distribution. Flow distribution can be adjusted by the air guide vane of the air conditioner to provide proper conditions for different AHW types.

Received by 7 June 2022  
Revised by 13 August 2022  
Accepted by 1 October 2022

## Keywords:

microclimate control room, IoT system, atmospheric water harvesting, computational fluid dynamics

## 1. Introduction

The atmospheric water harvesting (AWH) is one of the reliable and sustainable sources of fresh water. The moisture in the air is available everywhere even in landlocked areas where the water sources are far and not available to access [1]. The estimated water amount in the air is around 12,800 trillion liters [2]. The AWH by direct cooling is now practical and commercial products with a

criterion of climate, i.e. relative humidity (RH)  $> 30\%$  [3] and RH  $> 40\%$  [4], while the desiccant AWH with high capability is intensively developed [5]–[9] even in the arid and desert areas where the RH is less than 20%. Beyond water production, the desiccant AWH can be served as the electricity generation [10]–[12]. However, the desiccant AWH technology are still in the demonstration and proof of concept.

Most of previous studies for both AWH by direct cooling and desiccants were performed under the actual climates [4], [13]–[20], which is uncontrollable air temperature and RH. For example, a group of works tested the portable AWH system based on the thermoelectric cooler under ambient temperature and RH in the range of 18-30 °C and 60-82 %, respectively [17]. The results showed that water production rate was varied in a wide range of 2.7-40.3 mL/h. Kim et al [4] reported that the metal-organic framework (MOF)-801 can capture the water from air over 0.25 L/kg of MOF for a single daily cycle in the desert of Arizona, USA, where RH is 5% at 35 °C to 40 °C during the day and 40% at 10 °C to 15 °C during the night. MOF-801 also reported that it produced 100 g of water/kg of MOF-801 in the same desert, but MOF-303 delivered over 2 times of water capture [16].

From the literatures, AWHs by direct cooling or desiccants were claimed by the promising results under actual climate. However, those results are difficult to compare directly because of the difference of test conditions. This is a vulnerable spot of AWH research that tests under actual conditions. Only few works have studied AWH with the controlled climate conditions before going into the system inlet. Gong et al [12] have tested small amount of nature-based desiccant in a very small controllable microclimate chamber. RH can be varied from 20% to 80%, but details of the microclimate chamber were not revealed. With the simulated microclimate, the extreme conditions revealed more information of AWH at 20% to 80% RH. Hand and Peuker [21] used the ultrasonic humidifier to simulate a condition of moist air near 100%

RH for studying the effect of orientation of a thermoelectric device. He et al [22] also tested the performance and efficiency of AWH using thermoelectric devices with the simulated inlet air. Effect of RH and air flow rate on performance can be investigated separately as well as shown by Bagheri [2] that proposed a systematic method for assessment of the AWH performance and limitation with a commercially controllable environment chamber. The actual climate like conditions were simulated covering various climatic conditions, i.e. warm and humid (32 °C and 60% RH), mild and humid (20 °C and 75% RH), cold and humid (6 °C and 80% RH), warm and dry (32 °C and 20% RH), mild and dry (21 °C and 45% RH), cold and dry (6 °C and 57% RH) and mild (25 °C and 50% RH). After obtaining the desired condition, the simulated air was fed into the inlet of AWH devices. With variation of the simulated climatic conditions, they found the limitations and characteristics of the system.

Despite the aforementioned works controlled the climatic conditions, they only limited for the inlet of AWH devices. Other parts of AWH systems were still in different surrounding conditions. This could affect on the experimental results of AWH system in the viewpoint of energy efficiency. For example, heat transfer rate and energy consumption of the condenser were changed if the surrounding condition was different. This is a very real pain point for the AWH research. The simulated climate situation closing to the actual situation as much as possible is needed to analyze the system and gain a greater understanding of parameters. However, there is so far no work on the large microclimate control room for AWH research to fully test the entire AWH system.

This work proposes for the first time of the development of an innovative microclimate control room with the parallel control using IoT system to provide more realistic situation for AWH research. Flow and temperature distribution inside the microclimate control room were also assessed by computational fluid dynamics.

## 2. Methodology

### 2.1 Atmospheric Water Harvesting

The principle of atmospheric water harvesting is the condensation of moisture in air. The direct cooling and the vapor concentration using desiccants are promising techniques for AWH. Direct cooling method drives the water vapor to liquid by reduction of air temperature. For the direct cooling, high energy consumption and suitable relative humidity (>30% RH) are required, while the vapor concentration with desiccants requires lower energy consumption and lower relative humidity. For the vapor concentration, the additional processes, i.e. moisture collection and release, have to be performed before condensation. More details of both techniques are available in [5], [8], [23]. The important properties of moist air for AWHs are dry bulb temperature, specific humidity, relative

humidity and enthalpy of moist air. The correlation of these properties are shown in [23].

### 2.2 Setup of Microclimate Control Room

The microclimate control room consists of the control system, i.e. main controller units (MCU ESP32), a group of sensors for measuring temperature and relative humidity and an infrared transmitter (IR module), and equipment for microclimate change, i.e. air conditioner, heater, humidifier and dehumidifier, as shown in Fig. 1. The microclimate condition can be controlled by offline control or online control by the control panel of MCU or the Blynk IoT platform through the internet protocol, respectively. The IR module was only added at a position in the room to control the air conditioner.

Fig. 2 shows the actual alignment of microclimate control room following the setup diagram. The room dimensions are  $2.5 \times 4.5 \times 3$  m (W  $\times$  L  $\times$  H). Ten measurement points were distributed at 2 m height. Fans behind the 2500 W heater were operated at 150 rpm all the time during test. The capacities of air conditioner, humidifier and dehumidifier are 9,000 BTU, 4 L/h and 30 L/day, respectively. Before setup, the temperature and humidity sensors were compared with the reference thermometer and psychrometer under the range of operating conditions, i.e. temperature of 16-50 °C and relative humidity of 40-80%. The analog and I<sup>2</sup>C digital temperature and humidity complex sensors were used in this work to compare the accuracy (AMT1001 for analog sensor and AM2315 and SHT20 for digital sensor). For temperature measurement, analog signal temperature sensors (Lm 35) were also used to confirm data accuracy.

The design concept of the microclimate control system is shown in Fig. 3. At first, MCU receives the set temperature and humidity (SetTemp and SetHumi) from the user via the online application or control panel. The room temperature and humidity are averaged from a group of sensor nodes named as RoomTemp and RoomHumi, respectively. MCU compares the room temperature and humidity with the set temperature and humidity. If the RoomTemp is less than the SetTemp, the MCU is alerted to control the heater with the PID controller algorithm. If the RoomTemp is higher than SetTemp, the MCU controls an air conditioner with the same SetTemp values through the infrared light emitting diode (IR transmitter). To control the humidity in the room, the MCU compares the RoomHumi with the SetHumi. If the RoomHumi is less than the SetHumi, the MCU activates the humidifier. Conversely, the dehumidifier is operated when the RoomHumi is higher than SetHumi.

To assure that the control system of microclimate control room can operate consistently and stably, the assessment was divided into 2 parts. Short period of control with condition changing was firstly tested to observe system behavior at air temperature and relative humidity between 20-45 °C and 40-80%, respectively. Then long period tests were performed for 10 hours to check stability

of the system. The ambient temperature and humidity ratio outside the room were also measured to show the independence of control system. To find the average value for each condition, the experimental tests were performed in 5 repetitions.

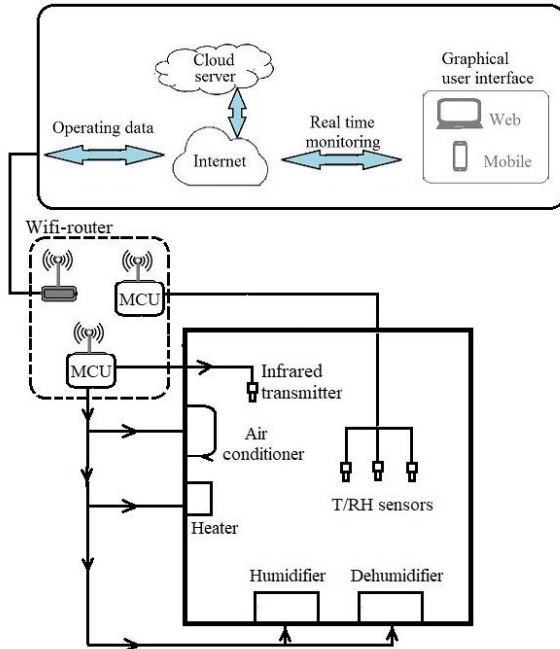


Fig. 1 The schematic diagram of microclimate control system

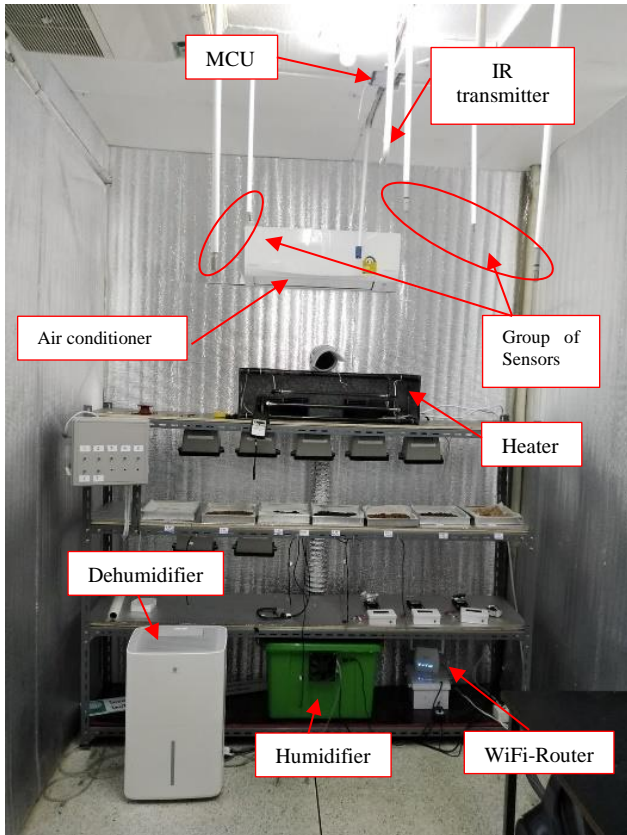


Fig. 2 The experimental prototype of the microclimate control room

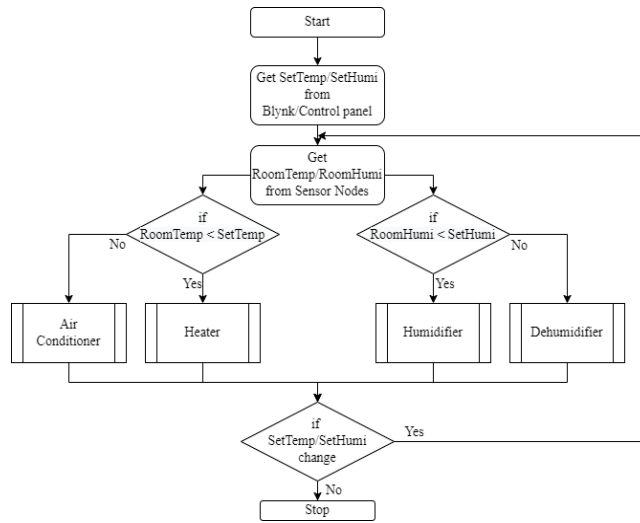


Fig. 3 Design concept of the microclimate control system

### 2.3 Air Flow Analysis of Microclimate Control Room

To investigate air flow distribution and obtain the optimal flow characteristic for testing under wide range of climate, air velocity and temperature distribution in microclimate control room can be assessed by the computational fluid dynamics. The governing equations used are following:

$$\frac{\partial \rho}{\partial t} + \nabla \cdot (\rho \mathbf{v}) = 0 \quad (1)$$

$$\frac{\partial}{\partial t} (\rho \mathbf{v}) + \nabla \cdot (\rho \mathbf{v} \mathbf{v}) = -\nabla p + \nabla \cdot (\boldsymbol{\tau}) + \rho \mathbf{g} + \mathbf{F} \quad (2)$$

$$\frac{\partial}{\partial t} (\rho E) + \nabla \cdot (\mathbf{v}(\rho E + p)) = \nabla \cdot (k_{eff} \nabla T) + S_h \quad (3)$$

Where  $\rho$ ,  $t$ ,  $\mathbf{v}$ ,  $p$ ,  $\boldsymbol{\tau}$ ,  $\mathbf{F}$ ,  $E$ ,  $k_{eff}$ ,  $T$  and  $S_h$  are density, time, flow velocity, pressure, stress tensor, gravity, momentum sink term, total energy, effective conductivity, temperature and volumetric heat source, respectively. The turbulent k- $\epsilon$  model was used for calculation as shown in [24]. To reduce the simulation complexity, assumptions of no-slip wall, steady state and incompressible flow condition are used. The model and grid cell of the microclimate control room for simulation are shown in Fig. 4 (a) and (b), respectively. Grid independent study was performed before air flow assessment. The optimum grid for flow simulation was 882,655 cells.

Model validation was performed by comparison of the experimental results and simulation at the same condition. A hot wire anemometer (Jedto-AFM029) was used to measure air velocities and temperatures with accuracy  $\pm 3\%$  and  $2\text{ }^{\circ}\text{C}$ , respectively, at the positions shown in Fig. 4 (c). Velocity and temperature for each point were acquired in triplicate.

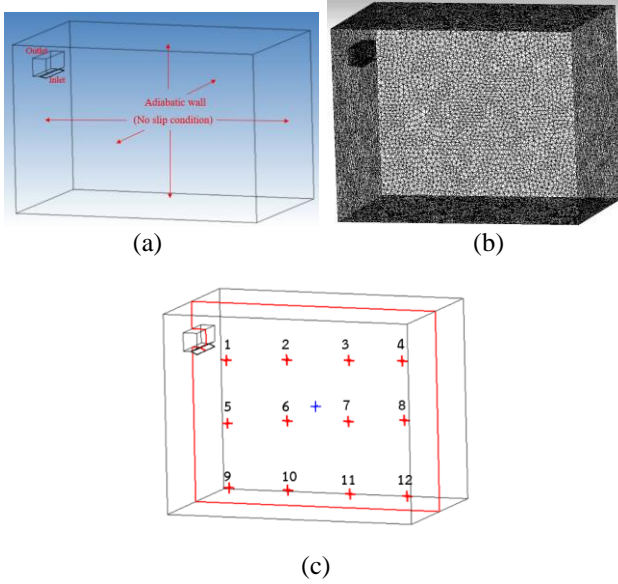


**Fig. 4** (a) Model of microclimate control room, (b) Model discretization and (c) Plane for visualization.

The boundary conditions for simulation in case of cooling and heating mode were referred to the actual operating condition. For cooling mode, the inlet was assigned as 21 °C and 3.5 m/s for air temperature and velocity, respectively, with the turbulence intensity of 2%. The angle of air inlet was varied horizontally by 15° from 30° to 90°. The atmospheric pressure and room temperature were used for the outlet. For heating mode, the inlet condition of heater was 50 °C and 3.5 m/s for prediction. The number of iterations of 5,000 cycles and the residual values of 0.0001 for all variables were the criteria for calculation [25].

### 3. Results and Discussion

#### 3.1 Sensor Calibration

The calibration curves of sensors were successfully constructed with the reference data of air temperature and relative humidity as shown in Fig. 5 and Fig. 6, respectively. It was revealed that air temperature and relative humidity measured by sensors increased linearly as reference values increased under desired conditions (air temperature of 15-50 °C and relative humidity of 40-80 %). The linear regression lines represent the calibration curves at measured values with high determination coefficients ( $R^2 > 0.98$ ). This could be expressed that the calibrated sensors are established using for air temperature and relative humidity in the range of calibration.

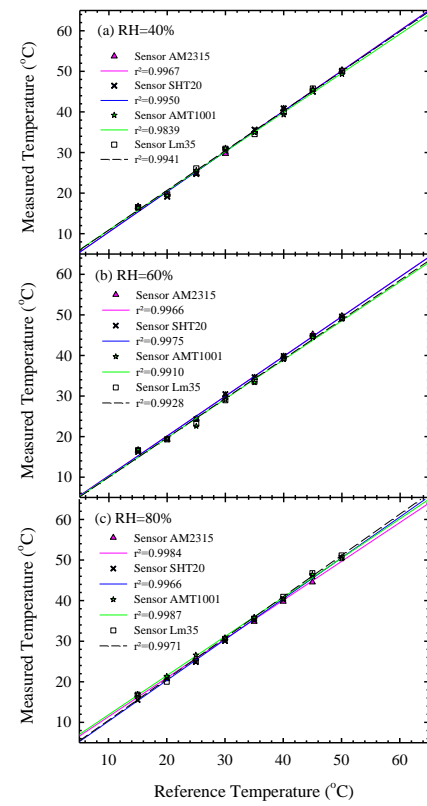


**Fig. 5** Calibration curves of temperature sensor under desired temperatures at different relative humidity.

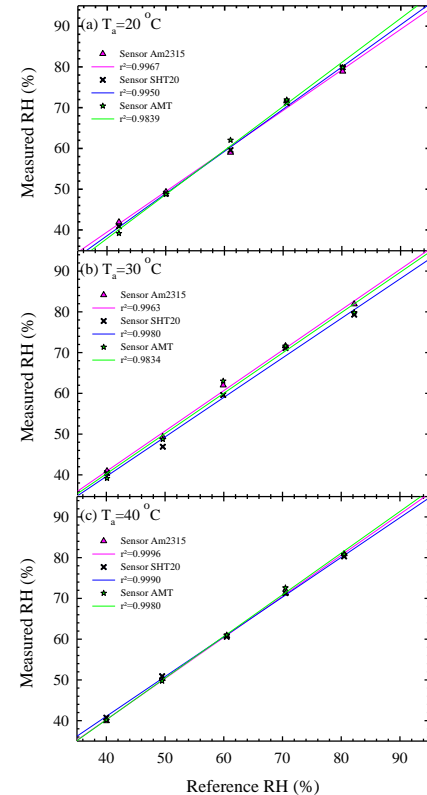


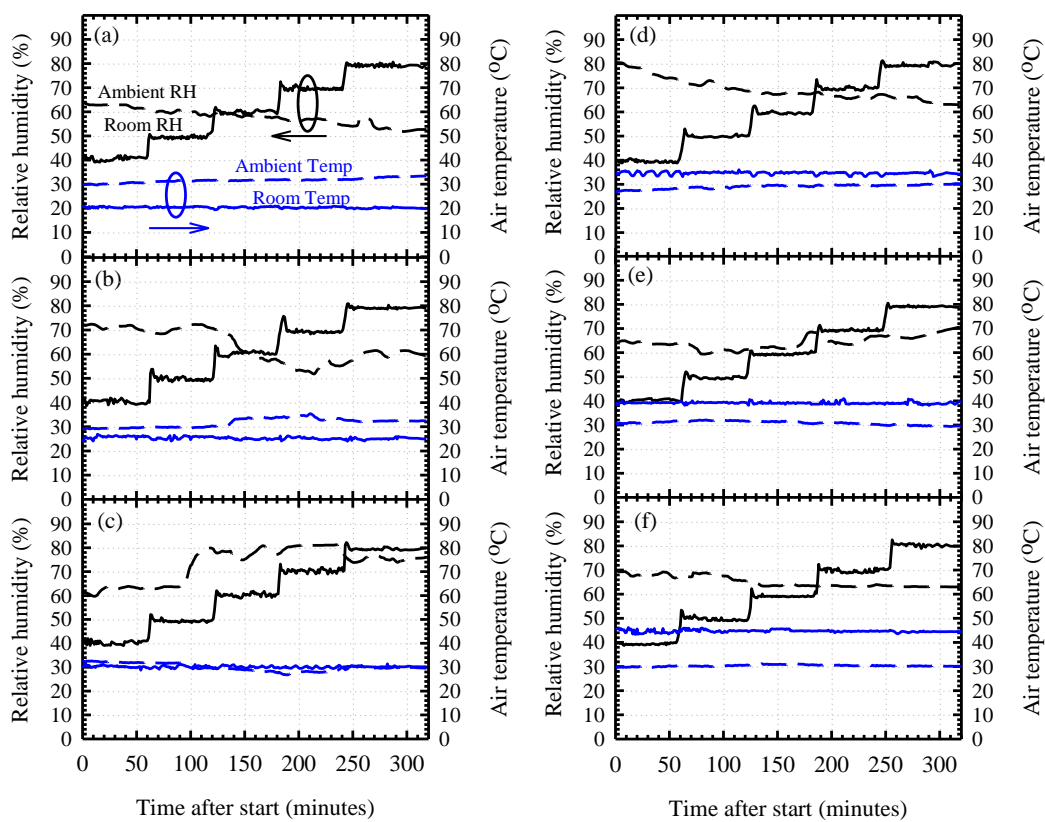
**Fig. 6** Calibration curves of relative humidity sensor under desired values at different temperature.

### 3.2 Microclimate Control

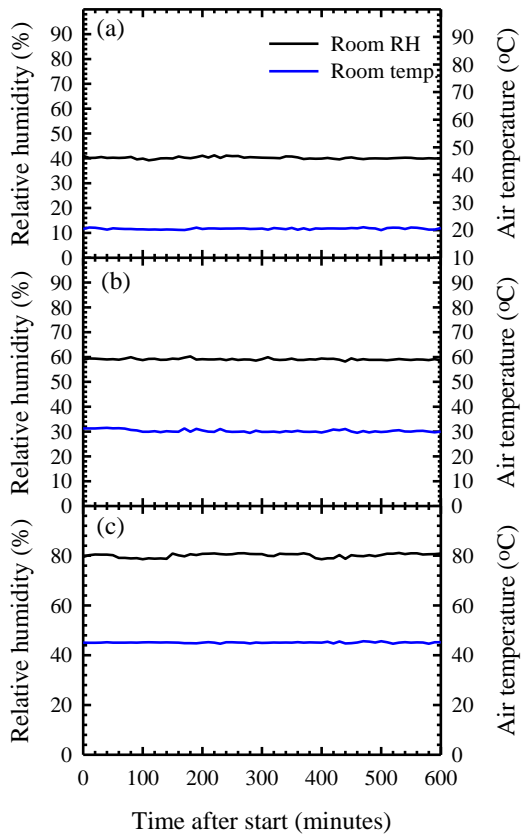
Short period test of microclimate control at desired conditions was shown in Fig. 7 to investigate the system before long operating control test. The results shown that the control system can constantly control the microclimate in the room for 60 minutes. Overshooting value of relative humidity can be observed at the beginning of new condition, but it can move to the set point and maintain consistently after 5 minutes as shown in Fig. 7 (a)-(f). The outside air temperature and relative humidity are also shown in the plots. It is clear that the control system can maintain the microclimate in the room without disturbance of the outside temperature and relative humidity

Fig. 8 shows temperature and relative humidity of long operating run tested at 30 °C and 60% RH for desired

condition, at 20 °C and 40% RH for the lowest limit and 45°C and 80% RH for the highest conditions, where the microclimate is difficult to be controlled. The control can maintain at target conditions with small fluctuation for 10 hours. With this result, the microclimate control room is available for parametric study of atmospheric water harvesting research. The parameters of microclimate control room can be varied individually for long test. However, a malfunction of the relay contact for dehumidifier was observed after 450 hours of operation, because of deterioration of the mechanism inside relay contact. To solve this problem, the relay contact was replaced by the opto-switch which is no moving part in the operation.



**Fig. 7** Test of microclimate control with relative humidity variation between 40-80 % in short period at a specific room temperature at (a) 20 °C, (b) 25 °C, (c) 30 °C, (d) 35 °C, (e) 40 °C and (f) 45 °C.



**Fig. 8** Long operating test at (a) lowest limit of control (20 °C and 40% RH) (b) desired condition (30 °C and 60% RH) and (c) highest limit (40 °C and 80% RH).

### 3.3 Air Flow and Temperature Distribution in Microclimate Control Room

The validation of model was performed by the comparison of experimental results and the simulations of velocity and temperature as shown in Fig. 9 (a) and (b), respectively. The validation showed that there is correlation between the experiment and simulation with the averaged relative error of 21.2% and 18.6% for velocity and temperature, respectively. The relative errors in this work are rated as B level and acceptable, according to Zhang et al. [26].

Air flow pattern in the microclimate control room was shown in Fig. 10. The different angle of air inlet resulted in different flow in the room. For AWH with direct desiccant, the 45° inlet angle seemed to have a proper location under the air conditioner, because the air velocity is low and there is no disturbance of air flow on the experiment. For AWH with direct cooling, the location at the middle room in case of the 30° inlet angle is suitable for the experiments, because more homogeneous velocity comparing with the others are available.

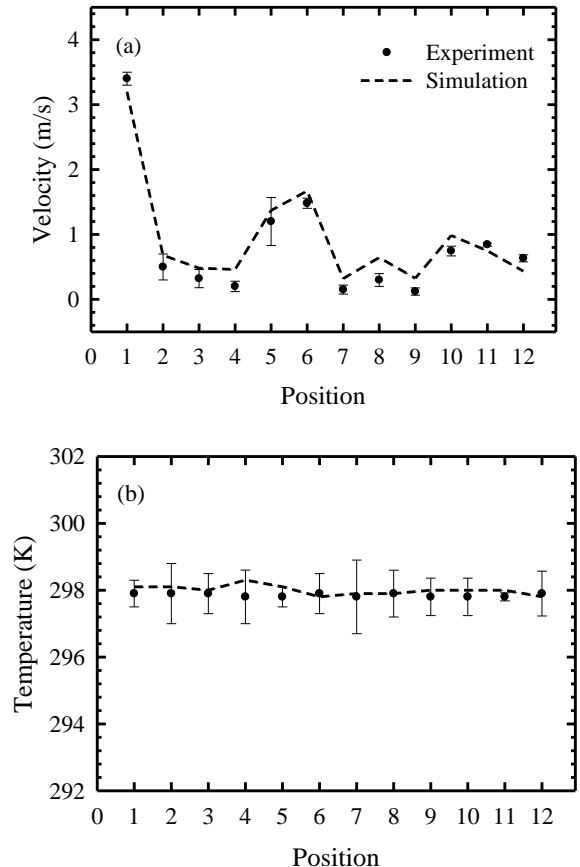


**Fig. 9** Model validation. (a) Velocity and (b) Temperature.

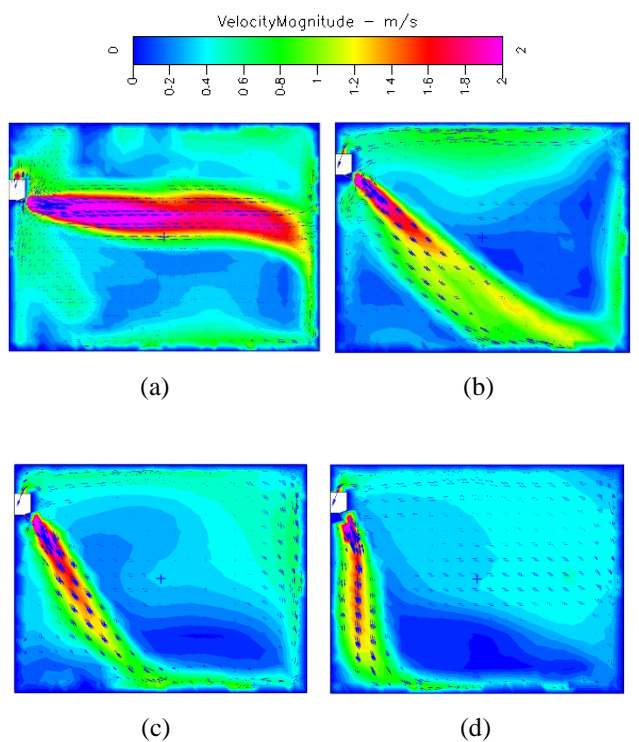


**Fig. 10** Flow pattern in the microclimate control room with different inlet angle at (a) 30°, (b) 45°, (c) 60° and (d) 90°.

Fig. 11 (a) and (b) show the temperature distribution in the microclimate control room in case of cooling mode with inlet temperature of 25 °C and heating mode with inlet temperature of 50 °C, respectively. Air temperature was homogeneously distributed in the control room for both cases. This condition control can be used for the experiments of AWH with direct cooling or desiccants. With the control system developing in this work, the sensitivity of parameters of AWH can be investigated separately.

## 4. Conclusion

This work presented a development of microclimate control room using IoT system to provide more realistic situation for atmospheric water harvesting research. A new test bed developed can vary the temperature and relative humidity between 20-45 °C and 40-80%, respectively. For short and long operations, the control system successfully operated and maintained the desired microclimate without the disturbance of ambient air. With the simple geometry of the room, the homogeneous temperature distribution was obtained by alignment of the operating devices. Flow distribution can be selected by adjusting the air guide vane of the air conditioner. The 45° inlet angle of the air guide vane provided the proper still air for AWH by direct desiccant at the position under the outlet of air conditioner, while of the 30° inlet angle provided homogeneous velocity distribution which is suitable for AWH by direct cooling. The opto-switch was suggested for using in the control system instead of the mechanical switch or relay contact.

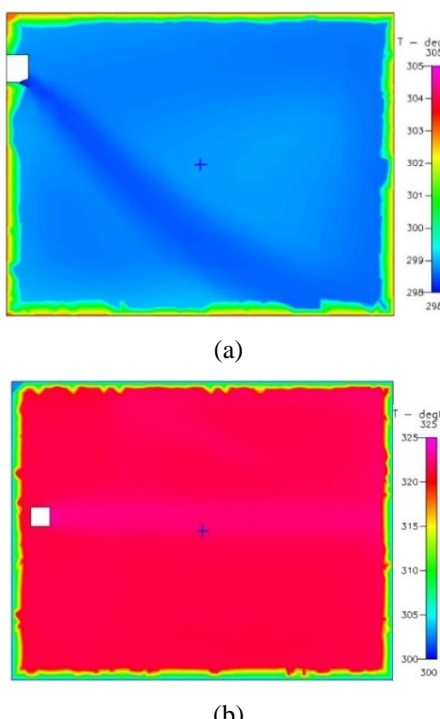


**Fig. 11** Temperature distribution (a) Cooling mode using air conditioner with air discharge temperature of 25 °C and (b) Heating mode using heater with air discharge temperature of 50 °C.

The extensions of this work in the future will deal with the parametric study to increase the energy efficiency, the novel AWH technologies and the optimization of AWH system under the simulated microclimate conditions before the field test.

## Acknowledgements

The financial support of this work was provided by the National Research Council of Thailand (NRCT) through the research and innovation grant (No. N25A650020).

## References

- [1] X. Zhou, H. Lu, F. Zhao, and G. Yu, "Atmospheric Water Harvesting: A Review of Material and Structural Designs," *ACS Mater. Lett.*, vol. 2, no. 7, pp. 671-684, Jul. 2020, doi: 10.1021/acsmaterialslett.0c00130.
- [2] F. Bagheri, "Performance investigation of atmospheric water harvesting systems," *Water Resour. Ind.*, vol. 20, pp. 23-28, Dec. 2018, doi: 10.1016/j.wri.2018.08.001.
- [3] A. A. Salehi, M. Ghannadi-Maragheh, M. Torab-Mostaedi, R. Torkaman, and M. Asadollahzadeh, "A review on the water-energy nexus for drinking water production from humid air," *Renew. Sustain. Energy Rev.*, vol. 120, pp. 109627, Mar. 2020, doi: 10.1016/j.rser.2019.109627.
- [4] H. Kim *et al.*, "Adsorption-based atmospheric water harvesting device for arid climates," *Nat. Commun.*, vol. 9, no. 1, pp. 1191, Dec. 2018, doi: 10.1038/s41467-018-03162-7.
- [5] K. Yang, T. Pan, Q. Lei, X. Dong, Q. Cheng, and Y. Han, "A Roadmap to Sorption-Based Atmospheric Water Harvesting: From Molecular Sorption Mechanism to Sorbent Design and System Optimization," *Environ. Sci. Technol.*, vol. 55, no. 10, pp. 6542-6560, May 2021, doi: 10.1021/acs.est.1c00257.
- [6] G. Raveesh, R. Goyal, and S. K. Tyagi, "Advances in atmospheric water generation technologies," *Energy Convers. Manag.*, vol. 239, p. 114226, Jul. 2021, doi: 10.1016/j.enconman.2021.114226.
- [7] R. Peeters, H. Vanderschaeghe, J. Rongé, and J. A. Martens, "Fresh water production from atmospheric air: Technology and innovation outlook," *iScience*, vol. 24, no. 11, p. 103266, Nov. 2021, doi: 10.1016/j.isci.2021.103266.
- [8] Y. Tu, R. Wang, Y. Zhang, and J. Wang, "Progress and Expectation of Atmospheric Water Harvesting," *Joule*, vol. 2, no. 8, pp. 1452-1475, Aug. 2018, doi: 10.1016/j.joule.2018.07.015.
- [9] Z. Chen *et al.*, "Recent progress on sorption/desorption-based atmospheric water harvesting powered by solar energy," *Sol. Energy Mater. Sol. Cells*, vol. 230, p. 111233, Sep. 2021, doi: 10.1016/j.solmat.2021.111233.
- [10] R. Li, M. Wu, S. Aleid, C. Zhang, W. Wang, and P. Wang, "An integrated solar-driven system produces electricity with fresh water and crops in arid regions," *Cell Rep. Phys. Sci.*, vol. 3, no. 3, p. 100781, Mar. 2022, doi: 10.1016/j.xcrp.2022.100781.
- [11] T. Ding, Y. Zhou, W. L. Ong, and G. W. Ho, "Hybrid solar-driven interfacial evaporation systems: Beyond water production towards high solar energy utilization," *Mater. Today*, vol. 42, pp. 178-191, Jan. 2021, doi: 10.1016/j.mattod.2020.10.022.
- [12] F. Gong *et al.*, "Agricultural waste-derived moisture-absorber for all-weather atmospheric water collection and electricity generation," *Nano Energy*, vol. 74, p. 104922, Aug. 2020, doi: 10.1016/j.nanoen.2020.104922.

- [13] J. S. Solís-Chaves, C. M. Rocha-Osorio, A. L. L. Murari, V. M. Lira, and A. J. Sguarezi Filho, "Extracting potable water from humid air plus electric wind generation: A possible application for a Brazilian prototype," *Renew. Energy*, vol. 121, pp. 102–115, Jun. 2018, doi: 10.1016/j.renene.2017.12.039.
- [14] A. Scrivani and U. Bardi, "A study of the use of solar concentrating plants for the atmospheric water vapour extraction from ambient air in the Middle East and Northern Africa region," *Desalination*, vol. 220, no. 1–3, pp. 592–599, Mar. 2008, doi: 10.1016/j.desal.2007.04.060.
- [15] M. Mirmanto, S. Syahrul, A. T. Wijayanta, A. Mulyanto, and L. A. Winata, "Effect of evaporator numbers on water production of a free convection air-water harvester," *Case Stud. Therm. Eng.*, vol. 27, p. 101253, Oct. 2021, doi: 10.1016/j.csite.2021.101253.
- [16] F. Fathieh, M. J. Kalmutzki, E. A. Kapustin, P. J. Waller, J. Yang, and O. M. Yaghi, "Practical water production from desert air," *Sci. Adv.*, vol. 4, no. 6, pp. eaat3198, Jun. 2018, doi: 10.1126/sciadv.aat3198.
- [17] I. Casallas, M. Pérez, A. Fajardo, and C.-I. Paez-Rueda, "Experimental Parameter Tuning of a Portable Water Generator System Based on a Thermoelectric Cooler," *Electronics*, vol. 10, no. 2, pp. 141, Jan. 2021, doi: 10.3390/electronics10020141.
- [18] M. Elashmawy and F. Alshammary, "Atmospheric water harvesting from low humid regions using tubular solar still powered by a parabolic concentrator system," *J. Clean. Prod.*, vol. 256, pp. 120329, May 2020, doi: 10.1016/j.jclepro.2020.120329.
- [19] M. Elashmawy, "Experimental study on water extraction from atmospheric air using tubular solar still," *J. Clean. Prod.*, vol. 249, pp. 119322, Mar. 2020, doi: 10.1016/j.jclepro.2019.119322.
- [20] M. Elashmawy and I. Alatawi, "Atmospheric Water Harvesting from Low-Humid Regions of Hail City in Saudi Arabia," *Nat. Resour. Res.*, vol. 29, no. 6, pp. 3689–3700, Dec. 2020, doi: 10.1007/s11053-020-09662-y.
- [21] C. T. Hand and S. Peuker, "An experimental study of the influence of orientation on water condensation of a thermoelectric cooling heatsink," *Heliyon*, vol. 5, no. 10, p. e02752, Oct. 2019, doi: 10.1016/j.heliyon.2019.e02752.
- [22] W. He, P. Yu, Z. Hu, S. Lv, M. Qin, and C. Yu, "Experimental Study and Performance Analysis of a Portable Atmospheric Water Generator," *Energies*, vol. 13, no. 1, p. 73, Dec. 2019, doi: 10.3390/en13010073.
- [23] R. Munsin *et al.*, "Feasibility Study of Atmospheric Water Harvesting by Direct Cooling in Thailand," in *The 6<sup>th</sup> International Conference on Green Technology and Sustainable Development, Nha Trang University, Nha Trang, Vietnam, July 29-30, 2022*.
- [24] V. Wang, A. Jadav, R. Munsin, and Y. Laounual, "Investigation of Pre-Injection Flow Characteristics in Constant Volume Combustion Chamber (CVCC) using Computational Fluid Dynamics (CFD)," in *The 5<sup>th</sup> TSME International Conference on Mechanical Engineering, The Empress, Chiang Mai, Thailand, December 17-19, 2014*.
- [25] M. Rakyat *et al.*, "Study of air distribution in tray dryer using computational fluid dynamics," *Eng. Appl. Sci. Res.*, vol. 48, no. 6, Art. no. 6, Jul. 2021.
- [26] Z. Zhang, W. Zhang, Z. J. Zhai, and Q. Y. Chen, "Evaluation of Various Turbulence Models in Predicting Airflow and Turbulence in Enclosed Environments by CFD: Part 2—Comparison with Experimental Data from Literature," *HVACR Res.*, vol. 13, no. 6, pp. 871–886, Nov. 2007, doi: 10.1080/10789669.2007.10391460.

## Biographies



**Ronnachart Munsin** is working at Rajamangala University of Technology Lanna (RMUTL). He received his D.Eng. in Mechanical Engineering from KMUTT in 2015, and worked as a postdoctoral fellow at the Université d'Orléans, France in 2016. His research focuses on atmospheric water harvesting and combustion.



**Autanan Wannachai** received the B.Eng. in Computer Engineering from RMUTL and the M.Eng. degree and Ph.D. in Computer Engineering, from Chiang Mai University, Thailand. His research interests include embedded systems, wireless sensor networks, early warning systems for disasters, and autonomous systems.



**Nopphadon chongbun** is working on his final year project with Dr. Ronnachart Munsin. He is a fourth-year undergraduate student at the Department of Mechanical Engineering, RMUTL. He focuses on microclimate control system.



**Satit Karnpian** is working on his project with Dr. Ronnachart Munsin. He is an undergraduate student at the Department of Mechanical Engineering, RMUTL. He focuses on natural-based composite desiccant performance.



**Nachapon Sumankant** is working on his project with Dr. Ronnachart Munsin. He is a B.Eng. student at the Department of Mechanical Engineering, RMUTL. He focuses on natural-based composite desiccant properties.



**Kanthanat Sanwong** is working on his final year project with Dr. Ronnachart Munsin. He is an undergraduate student at the Department of Mechanical Engineering. He focuses on flow simulation in the room using CFD.



**Settawut Pinta** is a first-year master student under the supervision of Dr. Ronnachart Munsin. His current research focuses on atmospheric water harvesting by hybrid system of direct cooling and desiccants.



**Jirasak Panya** received the M.Eng. in Mechanical Engineering from Chiang Mai University in 2009. Currently he is a lecturer at RMUTL. His research interests include machine design, refrigeration and air conditioning and fluid machinery.



**Pracha Yeunyongkul** received his D.Eng. in Mechanical engineering from Chiang Mai University in 2012. He is currently an associate professor at RMUTL. His research interests include application of heat pipe, heat exchanger design and geopolymers.



**Nawee Nuntapap** received his M.Eng. in Mechanical engineering from KMUTT in 2014. He is currently an assistant professor at RMUTL. His research interests include measurement and instrumentation and control



**Taweesak Mahawan** received his M.Eng. in Mechanical engineering from Chiang Mai University in 2010. He is currently a lecturer at RMUTL. His research interests include agricultural machinery and processes, energy conservation.



**Arpiruk Hokpunna** received his doctorate in Engineering from the Technical University of Munich in 2009. He is currently an assistant professor at Chiang Mai University. His research field includes numerical methods for fluid flow, industrial modeling, simulation and design as well as precision agriculture.



**Nattaporn Chaiyat** is working as an associate professor at Maejo University. He received his D.Eng. in Energy Engineering from Chiang Mai University, Thailand in 2011. His research interests focus on energy and renewable engineering.